

# Laser-induced cooling of broadband heat reservoirs

D. Gelbwaser-Klimovsky,<sup>1</sup> K. Szczygielski,<sup>2</sup> U. Vogl,<sup>3,\*</sup> A. Saß,<sup>3</sup> R. Alicki,<sup>2</sup> G. Kurizki,<sup>1</sup> and M. Weitz<sup>3</sup>

<sup>1</sup>Weizmann Institute of Science, 76100 Rehovot, Israel

<sup>2</sup>Institute of Theoretical physics and Astrophysics, University of Gdańsk, Poland

<sup>3</sup>Institut für Angewandte Physik der Universität Bonn, Wegelerstraße 8, 53115 Bonn, Germany

We explore, theoretically and experimentally, a method for cooling a broadband heat reservoir, via its laser-assisted collisions with two-level atoms followed by their fluorescence. This method is shown to be advantageous compared to existing laser-cooling methods in terms of its cooling efficiency, the lowest attainable temperature for broadband baths and its versatility: it can cool down any heat reservoir, provided the laser is red-detuned from the atomic resonance. It is applicable to cooling down both dense gaseous and condensed media.

PACS numbers: 37.10.De, 42.50.Wk, 34.90.+q, 05.90.+m

**Introduction** The advancement of quantum technologies is demanding new cooling methods [1–4] as a follow-up on existing laser cooling [5–9]. A cooling method is assessed by its cooling power, thermodynamic efficiency (ratio of the cooling-power to the absorbed power), the minimal temperature it allows and its applicability under diverse conditions. Here we examine these thermodynamic characteristics for a simple method we have previously introduced [10–13], whereby heat is transferred from a reservoir by laser-assisted collisions to two-level atoms, and is subsequently emitted via atomic fluorescence (Fig. 1a). This method, hereafter referred to as laser-induced collisional redistribution (LICORE), is shown to be advantageous compared to sideband cooling [7, 14], regarding the ability to cool down a *broadband* heat reservoir. This ability is put to an experimental test for a hot bath of helium in collisional equilibrium with rubidium atoms and shown to be in good agreement with theory.

The present work is essentially a thermodynamic analysis of the cooling experiment performed in [10–12]. Its aim is to compare theory and experiment in LICORE setups and focus on its main thermodynamic implications.

**Theory** The LICORE scheme consists of an ensemble of two-level atoms, driven by the laser, and permanently coupled by *elastic* collisions to a hot bath, and by spontaneous emission to a cold bath, the electromagnetic vacuum, which is effectively at zero-temperature (Fig. 1a).

For a hot bath at temperature  $T$ , the auto-correlation (coupling) spectrum,  $G_H(\omega) = \int_{-\infty}^{\infty} e^{i\omega t} \langle B_H(t) B_H(0) \rangle dt$  satisfies the detailed-balance (Kubo-Martin-Schwinger, KMS) condition [15]:  $G_H(\omega) = e^{\frac{\hbar\omega}{k_B T}} G_H(-\omega)$ ,  $B_H(t)$  being the bath operator in the interaction picture and  $k_B$  the Boltzmann constant. This detailed balance condition is akin to the Kennard-Stepanov ratio of absorption and emission rates [16–19]. The spectral shape of  $G_H(\omega)$  is immaterial to the occurrence of cooling, but its peak and width affect the cooling rate, as shown below.

The steady-state solution of the master equation (see Appendix A) defines an *effective temperature*  $T_{\text{TLA}}$ ,

which is a measure of the stationary atomic level-populations ratio  $\rho_{ee}/\rho_{gg}$ , where  $\rho_{ee(gg)}$  is the excited-(ground-) state population of the two-level atom (TLA). The heat-flow direction between the atoms and the hot bath is determined by  $T_{\text{TLA}}$ . For large and positive  $\Delta$ , i.e. *red detuning* from the atomic resonance ( $\Delta \gg g$ ), its Boltzmann factor satisfies

$$e^{-\frac{\hbar\Delta}{k_B T_{\text{TLA}}}} \equiv \frac{\rho_{ee}}{\rho_{gg}} = \frac{\Gamma_p e^{-\frac{\hbar\Delta}{k_B T}}}{\Gamma_p + \gamma} \leq e^{-\frac{\hbar\Delta}{k_B T}}, \quad (1)$$

where the collision-induced pumping rate is  $\Gamma_p = \left(\frac{2g}{\Delta}\right)^2 G_H(|\Delta|)$ .  $g$  is the laser-atom resonant coupling and  $\gamma$  is the spontaneous-emission rate. Hence, for  $\Delta \gg g > 0$ , the atoms are effectively colder ( $T_{\text{TLA}} < T$ ) than the hot bath. This is consistent with the expressions obtained from our general theory [13] for the heat current flowing from the hot bath to a two-level atom (see SI, Eq. (S20) for the exact expression)

$$J_H = \hbar\Delta \Gamma_p \frac{\gamma e^{-\frac{\hbar\Delta}{k_B T}}}{\gamma + \left(1 + e^{-\frac{\hbar\Delta}{k_B T}}\right) \Gamma_p} > 0. \quad (2)$$

Consequently, heat flows to the atoms, thereby cooling the hot bath, provided  $\Delta > 0$ , for *any*  $T$ ,  $\gamma$  and  $\Gamma_p$ . The asymmetry between cooling and heating rates **of the buffer gas** in LICORE, as confirmed by the experimental data (Fig. 2), is expressed by

$$\frac{-J_H(-\Delta)}{J_H(\Delta)} = e^{\frac{\hbar\Delta}{k_B T}}. \quad (3)$$

This asymmetry is a consequence of two factors: 1) For  $|\Delta| \gg g$  the coupling strength to the cold bath (electromagnetic field) is independent of the sign of  $\Delta$ . 2) The hot -bath (buffer gas) coupling to the TLA,  $G_H(\Delta)$ , satisfies the (KMS) detailed balance relation. The asymmetry in (3) conforms to the common intuition that it is easier to heat up than to cool down. LICORE can be understood as follows. Collisions broaden the atomic

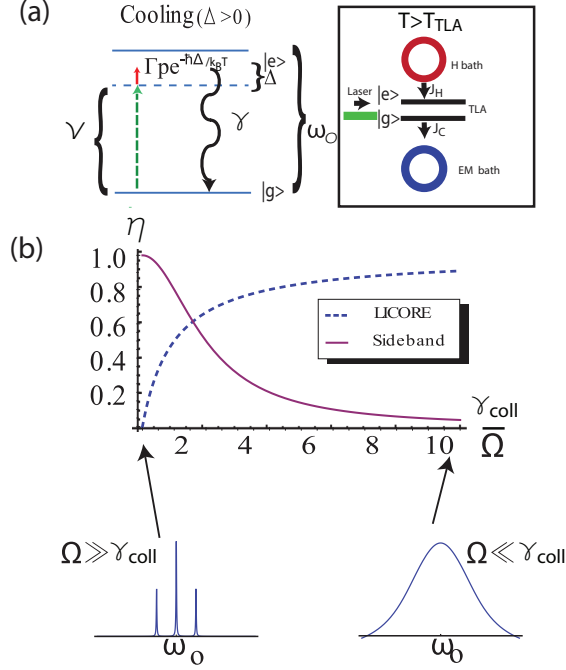


Figure 1. (Color online) (a) Schematic representation of cooling by laser-induced collisional redistribution (LICORE). Left– the level scheme along with the corresponding laser detuning  $\Delta$ , collisional pumping rate  $\Gamma_P$ , and the atomic spontaneous decay rate  $\gamma$ . Right– heat flow chart (TLA: two-level atom; EM: electromagnetic vacuum; H bath: hot bath; C bath: cold bath). (b) Sideband cooling compared to LICORE. Top: Efficiency as function of the band-width  $\gamma_{coll}$  scaled by  $\Omega$ . While sideband cooling (solid red line) is highly efficient for resolved sidebands ( $\Omega \gg \gamma_{coll}$ ), LICORE (dashed blue line) is much more efficient for unresolved sidebands ( $\Omega \ll \gamma_{coll}$ ). In sideband cooling  $\Omega$  is the trapping frequency, while in LICORE  $\Omega$  is the coupling Rabi frequency, taken to have the same value. The resolved sidebands spectrum conforms to the Mollow triplet [5–7].

levels, allowing the atom to absorb a photon below resonance frequency ( $\Delta = \omega_0 - \nu > 0$ ). Energy flow from the hot bath compensates for the energy mismatch between absorption at  $\nu$  and spontaneous emission at  $\omega_0$  to the electromagnetic vacuum (cold bath). The hot bath temperature is thereby reduced. In a perfectly isolated setup, this method would cool the hot bath down to *an arbitrarily low temperature*. As the hot bath temperature goes down, the cooling power in (2) is reduced but remains always positive. This is a salient advantage compared to both Doppler cooling [20, 21] and sideband cooling [7–9, 14] that have fundamental *minimal* cooling temperatures (see Table 1). The LICORE cooling efficiency is a product of two factors, corresponding to a two-step process: First, a photon is absorbed by the atom with

efficiency  $\frac{P_{abs}}{P_L}$ ,  $P_L$  being the incident laser power. Next, the absorbed photon drives the cooling with the thermodynamic efficiency  $\frac{J_H}{P_{abs}}$ . Thus the total efficiency in the weak laser limit ( $\Delta \gg g$ , using (2))

$$\eta = \frac{P_{abs}}{P_L} \frac{J_H}{P_{abs}} = \Delta \frac{\Gamma_p}{P_L} \frac{\gamma e^{-\frac{\hbar\Delta}{k_B T}}}{\gamma + \left(1 + e^{-\frac{\hbar\Delta}{k_B T}}\right) \Gamma_p}, \quad (4)$$

the absorbed power being (see SI)

$$P_{abs} = \hbar\nu \Gamma_p \frac{\gamma e^{-\frac{\hbar\Delta}{k_B T}}}{\gamma + \left(1 + e^{-\frac{\hbar\Delta}{k_B T}}\right) \Gamma_p}. \quad (5)$$

The extracted energy from the hot bath follows the detuning, and correspondingly the cooling power increases, for moderate detuning in the linear regime (Fig. 2). Yet, for large detuning laser absorption decreases, thereby reducing the cooling power. The highest efficiency is achieved if all photons are absorbed, ( $P_L = P_{abs} = \hbar\nu \Gamma_p \frac{\gamma}{\gamma + 2\Gamma_p}$ ), with unity efficiency being reached if the energy shift from the redistribution becomes as large as the entire cooling light photon energy,  $\hbar\nu$ , yielding  $J_H = P_{abs}$ . The efficiency of such a heat distributor can in principle be impressively high (Fig. 1b). On the other hand, optical transitions in atoms do not allow for reasonable absorption rates at detunings of order of the absolute photon energy, and a more typical value for the high pressure buffer gas broadened ensemble is a detuning of order of the thermal energy,  $\Delta \approx T$ , see Fig. 2, corresponding to  $\Delta \approx 10$  THz at 500 K gas temperature. This yields a typical efficiency  $J_H/P_{abs} \approx T/\omega_0$ .

To assess the merits of the LICORE method, we compare it (Table 1) to existing laser cooling methods: (i) *Doppler cooling*, which is based on the momentum change of an atom caused by the absorption and reemission of a photon [6]; (ii) *Sideband cooling* which takes advantage of the sidebands created by the interplay between internal and external degrees of freedom of a species [7] to reduce its trapped-state occupation by tuning a laser to the lower sideband. The latter method requires (Fig. 1b) the sidebands to be resolved, which amounts to strong binding to the trap  $\Omega \gg \gamma$ , otherwise heating processes will compete with the cooling. We can draw an analogy between the trapping frequency  $\Omega$  in sideband cooling and the coupling Rabi Frequency  $\Omega = \sqrt{4g^2 + \Delta^2}$  in LICORE since in both processes the modes to be cooled have frequency  $\Omega$ . Yet, we note that in LICORE the suppression of heating is achieved for any ratio of  $\gamma/\Omega$  provided there is *weak coupling* to the laser,  $g \ll \Delta$ , whence  $\Omega \simeq \Delta \left(1 + \frac{2g^2}{\Delta^2}\right)$ , since the heating probability is then proportional to  $\frac{2g^2}{\Delta^2}$ .

The thermodynamic efficiency bound determines the fraction of the absorbed energy used to cool down the

Table I. Comparison of performance

	$\Omega \ll \gamma$	$\Omega \gg \gamma$	Maximal thermodynamic efficiency $\left(\frac{J_H}{P_{\text{abs}}}\right)$
Doppler Cooling [20, 21]	$\frac{k_B T_{\text{min}}}{h\gamma} \approx 1/4$	$\frac{k_B T_{\text{min}}}{h\gamma} \approx 1/4$	$(m \text{ atom mass}) \frac{h\nu}{2c^2 m} \ll 1$
Sideband cooling [7–9, 14]	$\frac{k_B T_{\text{min}}}{h\Omega} \approx \frac{1}{\log\left(\frac{1+\gamma/4\Omega}{\gamma/4\Omega}\right)} \gg 1$	$\frac{k_B T_{\text{min}}}{h\Omega} \approx \frac{1}{\log\left(\frac{1+\gamma^2/16\Omega^2}{\gamma^2/16\Omega^2}\right)} \ll 1$	Resolved bands $\frac{\Omega}{\nu} = \frac{\Omega}{\omega_0 - \Omega} \lesssim 1$ Unresolved bands $\frac{\Omega}{\nu} = \frac{\Omega}{\omega_0 - \Omega} \ll 1$
Laser-induced collisional redistribution (LICORE)	$\frac{k_B T_{\text{min}}}{h\Omega} \approx \frac{1}{4 \log\left(\frac{\Delta}{g}\right)} \ll 1$	$\frac{k_B T_{\text{min}}}{h\Omega} \approx \frac{1}{4 \log\left(\frac{\Delta}{g}\right)} \ll 1$	Unresolved bands $\frac{\Omega}{\nu} \sim \frac{\Delta}{\nu} \lesssim 1$

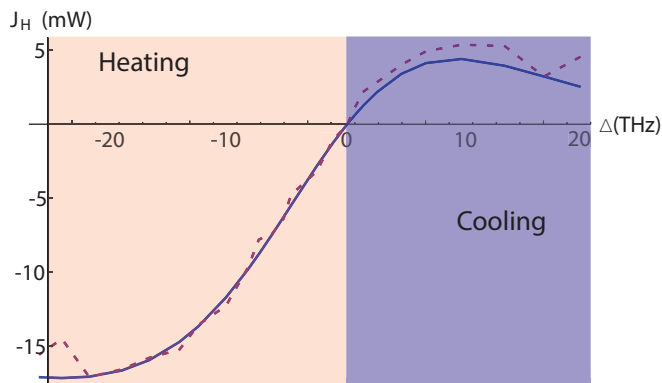


Figure 2. (Color online) Experimental results (red dashed line) compared to theoretical prediction (blue solid line) of the total cooling power as a function of the laser detuning  $\Delta$ . The y-axis indicates the cooling power. For red detuning,  $J_H$  corresponds to buffer gas cooling (purple, dark area), while blue detuning results in negative  $J_H$ , namely, buffer gas heating (orange, light area).

bath. The Doppler cooling efficiency is low, because it scales with the recoil parameter. Sideband cooling and LICORE cooling may achieve similar efficiency for an *extremely narrowband* oscillator bath, the scenario foreseen by sideband cooling, but LICORE may be highly efficient for a broadband bath, while sideband cooling efficiency will then be very low (Fig. 1b).

**Experiment** The cooling setup of a high pressure cell with optical access contains a mixture of atomic rubidium vapor, with number density on the order of  $10^{16} \text{cm}^{-3}$ , and a noble buffer gas that serves as the hot bath, here helium gas with a number density of  $1.5 \cdot 10^{21} \text{cm}^{-3}$  to  $6 \cdot 10^{21} \text{cm}^{-3}$ . The cell temperature is kept around 500 K.

The confocal optical setup shown in Fig. 3 is designed to characterize the spectral shift of the emitted fluorescence relative to the incident laser frequency. The collected atomic fluorescence radiation was analyzed with an optical spectrometer. Typical experimental data for an excitation laser frequency of 360 THz (401 THz), which is red (blue) detuned with respect to the D-lines resonances

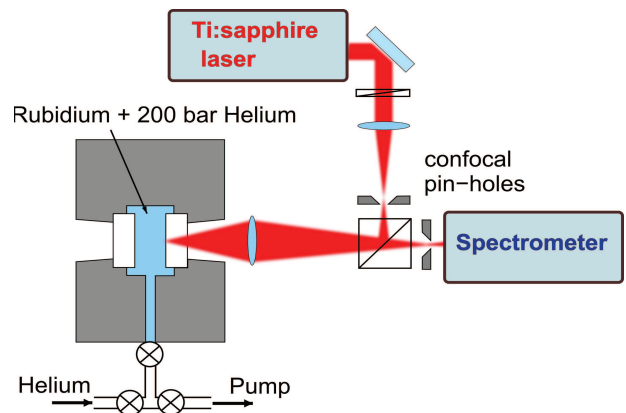


Figure 3. Experimental setup for confocal spectroscopy on high pressure helium-rubidium gas mixtures.

of the rubidium atoms, is shown in Fig. 4. The data displays typical pressure broadened fluorescence spectra, with the atomic rubidium D1- and D2-lines clearly visible, along with residual peaks of the exciting laser light. The figure clearly shows the redistribution of the fluorescence frequency to the center of the D-lines for both red and blue detuning respectively.

The cooling experiment is performed with a beam power of  $P_L = 2.4 \text{ W}$  on a 1 mm beam diameter. On resonance, the measured optical density in the 1 cm long gas cell, as derived from the transmitted laser power, reaches its maximum value of ca. 5. A more detailed description of the experimental setup and the characterization of the system can be found in [11].

In the present analysis we use experimental data for helium [12] instead of argon [10] as a buffer gas, as the thermal properties of helium, i.e. thermal conductivity and heat capacity differ both by an order of magnitude from the respective values in argon. Our theoretical model shows for both cases (helium and argon) excellent agreement with the experimental data, which demonstrates that the physical mechanism of cooling here is largely independent of those quantities. Helium, due to its higher

thermal conductivity may be better suited than other noble gases to couple the cooling scheme to a cooling load.

**Comparison of theory and experiment** We have measured the center of the fluorescence line and  $a(\nu)$ , the photon absorption probability. Upon identifying  $P_{\text{abs}} \equiv P_L a(\nu)$ ,  $J_H = P_L a(\nu) \frac{d}{\nu}$ . We relate the theoretical cooling power, Eqs (2) - (5), to its experimental counterpart. In our comparison, we account for laser absorption by many rubidium atoms in the cell.

The total cooling power can be calculated as:  $J_{H,\text{tot}} = \frac{N_a}{L} \int_0^L e^{-\alpha z} J_H(z) dz$ , where  $N_a/L$  is the linear rubidium atomic density, and the laser power is assumed to exponentially decay with  $z$  along the cell due to absorption. For a typical cooling laser frequency of 365 THz, the measured total absorption in the cell is 67%, corresponding to an absorption length  $l_{\text{abs}} \equiv 1/\alpha \simeq 9$  mm.

A quantitative comparison with theory requires an ansatz for the coupling (autocorrelation) spectrum to the buffer gas bath, the simplest being a *constant function*:  $G_H(\omega > 0) = G_H(0)$ . This ansatz means that the spectrum of collisions that couple the buffer gas and the rubidium atoms is *flat* within the absorption lineshape of the laser, i.e. collisional effects are independent of  $\Delta$ . The factor  $G_H(0)$  is determined from experimental data. We are aware that a more refined theory should account for the quasimolecular potential curves of rubidium-helium atom pairs [22]. Clearly, heat leakage (non-isolation) or molecule formation in the collisions may stop the cooling. Experimentally, much lower temperatures are attainable provided that the cooling region is well isolated from heat leakage.

Figure 2 compares the theoretical (blue solid line) and measured (red dashed line) cooling power. As predicted, the buffer gas (hot bath) is cooled down or heated up for red-detuned or blue-detuned laser, respectively. The difference between the measured and calculated curves reflects the difficulty to precisely determine the number of atoms to which the cooling power is proportional. Nevertheless, the main experimental features, i.e. the cooling and heating range and their asymmetry, are in very good agreement with theory.

**Minimal temperature predictions** In principle much lower temperatures are attainable by LICORE than those observed by us, provided the technical issues discussed above are experimentally addressed. We again emphasize that the present theory does not account for quasimolecular character of the alkali-noble gas system. LICORE cooling may reach lower temperatures than sideband or Doppler cooling, including ultralow temperatures ( $\frac{k_B T_{\text{min}}}{\hbar \Omega} \ll 1$ ) for both narrow and broadband spectra. Namely,  $\Omega \simeq \Delta$ , can be either narrow or broad compared to  $\gamma$  and still yield very low temperatures, while sideband cooling can reach such temperature only for resolved sidebands (Table 1)  $\Omega \gg \gamma$ . Our theory predicts that for a given value of  $\Omega$  at large detunings LICORE

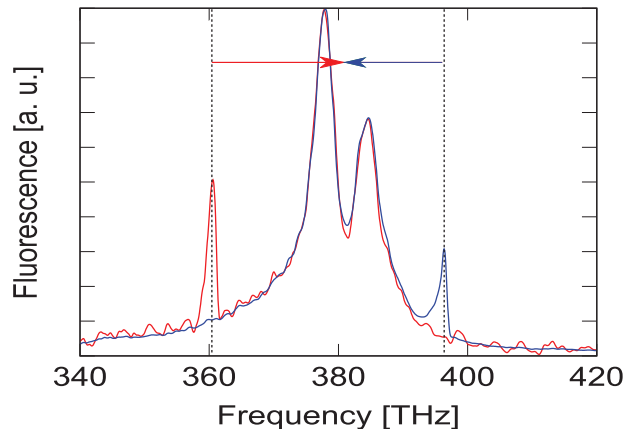


Figure 4. (Color online) Fluorescence spectra for rubidium vapor at 530 K with 200 bar helium buffer gas for excitation frequency 360 THz (red) and 401 THz (blue). Arrows indicate the direction of the mean frequency shift of the scattered photons by the redistribution process towards the D-lines center.

may reach lower temperature than Doppler cooling (Table 1).

In a perfectly isolated cell cooling stops only when  $J_H = 0$  at the minimum buffer gas temperature obtainable from the *exact* expression (SI)

$$e^{-\frac{\Omega}{T_H}} = \frac{\delta_+ e^{-\frac{\nu_+}{T_C}} + \delta_-}{\delta_+ + \delta_- e^{-\frac{\nu_-}{T_C}}} \quad (6)$$

where the following short-hand notation is used:  $\nu_{\pm} = \nu \pm \Omega$ ,  $\delta_{\pm} = \left(\frac{\Omega \pm \Delta}{2\Omega}\right)^2 \frac{(\nu_{\pm})^3}{\omega_0^3} \gamma$ . For a weak laser and positive detuning ( $0 < g \ll \Delta \ll \nu$ ),  $\nu_+ \approx \omega_0$  and  $1 \gg \frac{\delta_-}{\delta_+} \gg e^{-\frac{\nu_+}{T_C}}$ , the minimal temperature attains the value  $\frac{k_B T_{\text{min}}}{\hbar \Omega} \approx \frac{1}{4 \log(\frac{\Delta}{g})}$  (see Table I). However, the LICORE cooling efficiency and rate are very low at such large detunings, as seen from Eqs. (4) and (5) (Fig. 1b).

**Discussion** The main advantage of LICORE is that both the efficiency and the minimum temperature are *adjustable by tunable laser parameters*,  $\Delta$  and  $g$ , while for Doppler or sideband cooling they depend on fixed parameters, spontaneous emission rate  $\gamma$  and trapping frequency  $\Omega$ . Furthermore, LICORE cooling does not impose any restriction on either the hot- or cold- bath spectra, and is linear in the laser power. It thus stands in stark contrast to refrigeration models [23, 24] where not only the modulation rate has to be above a critical rate, but also non-overlapping (resolved) hot and cold bath spectra are required [23]. However, the present scheme is a *heat distributor and not a refrigerator*, as it cools down the hot bath (rather than the cold bath) at the expense of the laser power. Without the laser irradiation, the effect of collisions with the bath would only be to decohere the atoms, rather than change the bath temperature.

Our combined experimental and theoretical results offer new fundamental and applied insights into the problem of laser-induced cooling of a heat bath. The fundamental insight is that it is possible to run a laser-driven cooler that is not constrained by the thermodynamic bounds governing a refrigerator or a sideband cooler, and therefore allows cooling a broadband bath down to much lower temperature, and uniquely high efficiency. The applied insight is that a new technological avenue may be opened for cooling diverse gaseous or condensed media by laser-driven two-level atoms. Namely, the present method can in principle bypass the limitations of currently used Doppler or sideband cooling methods in terms of performance and versatility: the technique does not resort to *auxiliary* atomic levels or to *resolvable sidebands*; it allows for *arbitrary* (particularly, broadband) bath spectra and temperatures and only requires a red detuning of the cooling laser.

**Acknowledgments** We acknowledge the support of ISF and BSF (G.K.), CONACYT (D.G.) the DFG, grant no. We1748-15 (U.V., A.S., M.W.) and the Foundation for Polish Science (TEAM project) co-financed by the EU (K.S. and R.A.) and the University of Gdansk, grant no. 538-5400-B166-13 (K.S.).

---

\* Present address: Max Planck Institute for the Science of Light, Günther-Scharowsky-Straße 1, Bau 24, 91058 Erlangen, Germany.

- [1] J. M. Taylor, A. S. Sørensen, C. M. Marcus, and E. S. Polzik, Phys. Rev. Lett. **107**, 273601 (2011).
- [2] A. Ruschhaupt, J. G. Muga, and M. G. Raizen, J. Phys. B: At. Mol. Opt. Phys. **39**, 3833 (2006).
- [3] N. Erez, G. Gordon, M. Nest, and G. Kurizki, Nature **452**, 724 (2008).
- [4] P. Domokos and H. Ritsch, Phys. Rev. Lett. **89**, 253003 (2002).
- [5] S. Chu, C. Cohen-Tannoudji, and W. Phillips, Rev. Mod. Phys. **70**, 685 (1998).
- [6] M. Sheik-Bahae and R. I. Epstein, Nature Photonics **1**, 693 (2007).
- [7] A. Schliesser, R. RiviÅšre, G. Anetsberger, O. Arcizet, and T. J. Kippenberg, Nature Physics **4**, 415 (2008).
- [8] R. I. Epstein, M. I. Buchwald, B. C. Edwards, T. R. Gosnell, and C. E. Mungan, Nature **377**, 500 (2002).
- [9] C. E. Mungan, M. I. Buchwald, B. C. Edwards, R. I. Epstein, and T. R. Gosnell, Phys. Rev. Lett. **78**, 1030 (1997).
- [10] U. Vogl and M. Weitz, Nature **461**, 70 (2009).
- [11] U. Vogl, A. Sass, S. Hasselmann, and M. Weitz, Journal of Modern Optics **58**, 1300 (2011).
- [12] U. Vogl, A. Sass, and M. Weitz, Proc. SPIE **8275**, 827508 (2012); arXiv:1209.2465.
- [13] K. Szczygielski, D. Gelbwaser-Klimovsky, and R. Alicki, Phys. Rev. E **87**, 012120 (2013).
- [14] H. G. Dehmelt, Nature **262**, 777 (1976).
- [15] H.-P. Breuer and F. Petruccione, *The theory of open*

*quantum systems* (Oxford, New York, USA, 2002).

- [16] E. Kennard, Physical Review **11**, 29 (1918).
- [17] B. Stepanov, *Soviet Physics Doklady*, **2**, 81 (1957).
- [18] J. R. Lakowicz, *Principles of Fluorescence Spectroscopy* (Kluwer Academic/Plenum Publishers, 1999).
- [19] P. Moroshkin, L. Weller, A. Sass, J. Klaers, and M. Weitz, Arxiv:1401.0731 (2014).
- [20] T. W. Hänsch and A. L. Schawlow, Optics Communications **13**, 68 (1975).
- [21] D. J. Wineland and W. M. Itano, Physical Review A **20**, 1521 (1979).
- [22] N. Allard and J. Kielkopf, Rev. Mod. Phys. **54**, 1103 (1982).
- [23] D. Gelbwaser-Klimovsky, R. Alicki, and G. Kurizki, Phys. Rev. E **87**, 012140 (2013).
- [24] M. Kolář, D. Gelbwaser-Klimovsky, R. Alicki, and G. Kurizki, Phys. Rev. Lett. **109**, 090601 (2012).

## APPENDIX

### A. Master Equation

The total Hamiltonian is given by

$$H = H_S(t) + \sum_{j=H,C} [(H_{SB})_j + (H_B)_j], \quad (\text{A1})$$

where the  $(H_B)_J$  is the  $j$ -bath free Hamiltonian. Here the laser-driven system Hamiltonian is:

$$H_S(t) = \frac{\hbar}{2}\omega_0\sigma_Z + \hbar g(\sigma_+e^{-i\nu t} + \sigma_-e^{i\nu t}), \quad (\text{A2})$$

where  $\omega_0$  is the (resonance) frequency of the two-level atom,  $\sigma_Z$  and  $\sigma_{\pm} = \sigma_X \pm i\sigma_Y$  are the appropriate spin-1/2 operators,  $\nu$  is the laser frequency and  $g$  is the coupling strength between the laser and the two-level atom. The laser detuning is  $\Delta = \omega_0 - \nu$ . The two-level atom coupling to the hot bath (H), via elastic collisions that do not change the two-level atom level populations, is described by

$$(H_{SB})_H = \hbar\sigma_Z \otimes B_H, \quad (\text{A3})$$

where  $B_H$  is the buffer gas bath operator. The coupling to the cold (C) bath (electromagnetic vacuum) via spontaneous emission is given by

$$(H_{SB})_C = \hbar\sigma_X \otimes B_C, \quad (\text{A4})$$

$B_C$  being the electromagnetic bath operator.

At steady-state, we may replace (A2) of the main text by the *averaged Hamiltonian*

$$\bar{H}_S = \frac{\hbar}{2}\Delta\sigma_Z + \hbar g\sigma_X, \quad (\text{A5})$$

where  $\Delta = \omega_0 - \nu$  expresses the laser detuning. Then the coupling operator to the  $j$ th bath,  $S_j$ , is decomposed into a Fourier series

$$S_j(t) = U^\dagger(t)S_j U(t) = \sum_{q=0,\pm 1,\pm 2,\dots \in \mathbf{Z}} \sum_{\{\bar{\omega}\}} S_{j,q}(\bar{\omega})e^{-i(\bar{\omega}+q\nu)t}, \quad (j = H, C) \quad (\text{A6})$$

The master equation has the following form with the Lindblad generator decomposed in a Floquet (harmonic) series

$$\dot{\rho}_S = \mathcal{L}\rho_S, \quad \mathcal{L} = \sum_{j=H,C} \sum_{q=0,\pm 1,\pm 2,\dots} \sum_{\bar{\omega}} \mathcal{L}_{q\bar{\omega}}^j, \quad (\text{A7})$$

$$\begin{aligned} \mathcal{L}_{q\bar{\omega}}^j \rho = & \\ \frac{1}{2} \{ & G_j(\bar{\omega} + q\nu) ([S_{j,q}(\bar{\omega})\rho, S_{j,q}^\dagger(\bar{\omega})] + [S_{j,q}(\bar{\omega}), \rho S_{j,q}^\dagger(\bar{\omega})]) + \\ & G_j(-\bar{\omega} - q\nu) ([S_{j,q}^\dagger(\bar{\omega})\rho, S_{j,q}(\bar{\omega})] + [S_{j,q}^\dagger(\bar{\omega}), \rho S_{j,q}(\bar{\omega})]) \}. \end{aligned} \quad (\text{A8})$$

Explicitly, in terms of  $\Omega = \sqrt{4g^2 + \Delta^2}$ , the laser-induced Rabi frequency, these coupling operators have the form

$$\begin{aligned} S_C(\nu - \Omega) &= \frac{\Delta - \Omega}{2\Omega} \begin{pmatrix} 0 & 1 \\ 0 & 0 \end{pmatrix}, \quad S_C(\nu) = \frac{g}{\Omega} \begin{pmatrix} 1 & 0 \\ 0 & -1 \end{pmatrix}, \\ S_C(\nu + \Omega) &= \frac{\Delta + \Omega}{2\Omega} \begin{pmatrix} 0 & 0 \\ 1 & 0 \end{pmatrix}. \end{aligned} \quad (\text{A9})$$

By contrast

$$S_H(0) = \frac{\Delta}{\Omega} \begin{pmatrix} 1 & 0 \\ 0 & -1 \end{pmatrix}, \quad S_H(\Omega) = \frac{2g}{\Omega} \begin{pmatrix} 0 & 0 \\ -1 & 0 \end{pmatrix}. \quad (\text{A10})$$

The heat currents flowing out of the  $j$ -th bath, which are the main observables of interest, obey the same harmonic (Floquet) expansion. They are given by

$$J_j(t) = \sum_{q=-1,0,1} \sum_{\bar{\omega}} J_{q\bar{\omega}}^j(t). \quad (\text{A11})$$

$$J_{q\bar{\omega}}^j(t) = -k_B T_j \text{Tr}[(\mathcal{L}_{q\bar{\omega}}^j(t)\rho(t)) \ln \tilde{\rho}_{q\bar{\omega}}^j(t)], \quad (\text{A12})$$

$$\tilde{\rho}_{q\bar{\omega}}^j = \frac{\exp\left\{-\frac{(\bar{\omega}+q\nu)\bar{H}}{\bar{\omega}k_B T_j}\right\}}{\text{Tr} \exp\left\{-\frac{(\bar{\omega}+q\nu)\bar{H}}{\bar{\omega}k_B T_j}\right\}}. \quad (\text{A13})$$

The absorbed power is

$$P_{abs} = -J_C(t) - J_H(t) \quad (\text{A14})$$

The population probabilities for the two-level atoms satisfy the following Markovian master equation (in the interaction picture)

$$\frac{d\rho_{ee}}{dt} = -(\Gamma_p + \gamma)\rho_{ee} + \Gamma_p e^{-\frac{\hbar|\Delta|}{k_B T}} \rho_{gg} \quad \Delta > 0 \quad (\text{A15})$$

and for negative detuning

$$\frac{d\rho_{ee}}{dt} = -\Gamma_p \rho_{ee} + (\Gamma_p e^{-\frac{\hbar|\Delta|}{k_B T}} + \gamma)\rho_{gg} \quad \Delta < 0 \quad (\text{A16})$$

At steady-state Eq. (A15) yields Eq. (1) of the main text.

## B. Heating regime

It is instructive to consider, for comparison sake, the heating regime obtained for  $\Delta < 0$ . In this regime  $T_{TLA}$  is determined by

$$e^{-\frac{\hbar|\Delta|}{k_B T_{TLA}}} \equiv \frac{\rho_{ee}}{\rho_{gg}} = \frac{\Gamma_p e^{-\frac{\hbar|\Delta|}{k_B T}} + \gamma}{\Gamma_p} \geq e^{-\frac{\hbar|\Delta|}{k_B T}}. \quad (\text{A17})$$

In this case the atoms are hotter ( $T_{TLA} > T$ ) than the hot bath, thus the heat flows from the atoms, heating up the bath. In this case, the absorbed photons have more energy than the spontaneously emitted photons ( $\omega_0 > \nu$ ) and the extra energy is absorbed by the bath, heating it up. The heat current is then

$$J_H = -\hbar|\Delta|\Gamma_p \frac{\gamma}{\gamma + \left(1 + e^{-\frac{\hbar|\Delta|}{k_B T}}\right)\Gamma_p} < 0. \quad (\text{A18})$$

The physical process is similar to that in the cooling case except that the Boltzmann factor in (2) of the main text is here absent, causing an asymmetry of the cooling and heating rates;

## C. Minimum temperature

The most general expression for the heat current flowing from the hot bath is [13]

$$J_H = N_a \Omega \Gamma_p \frac{e^{-\frac{\Omega}{T_H}} (\delta_+ + \delta_- e^{-\frac{\nu_-}{T_C}}) - (\delta_+ e^{-\frac{\nu_+}{T_C}} + \delta_-)}{\delta_- \left(1 + e^{-\frac{\nu_-}{T_C}}\right) + \delta_+ \left(1 + e^{-\frac{\nu_+}{T_C}}\right) + \left(1 + e^{-\frac{\Omega}{T_H}}\right)\Gamma_p}. \quad (\text{A19})$$

Under the conditions specified for Eq. (6)

$$e^{-\frac{\Omega}{T_H}} \approx \frac{\delta_-}{\delta_+} = \left(\frac{\Omega - \Delta}{\Omega + \Delta}\right)^2 \left(\frac{\nu_-}{\nu_+}\right)^3 \approx \left(\frac{2\left(\frac{g}{\Delta}\right)^2}{1 + \frac{\Omega}{\Delta}}\right)^2 \left(\frac{\nu_-}{\nu_+}\right)^3 \approx \left(\frac{g}{\Delta}\right)^4 \quad (\text{A20})$$

#### D. Experimental setup

The setup is shown in the main text (Fig. 3). It is a high pressure cell with optical access. It contains a mix-

ture of atomic rubidium vapor (whose density is of the order of  $10^{16}\text{cm}^{-3}$ ) with helium gas (whose density goes from  $1.5\cdot 10^{21}\text{cm}^{-3}$  to  $6\cdot 10^{21}\text{cm}^{-3}$ ). The cell walls are kept at around 500K. They are an extra heating source and its thermal contact with the buffer gas precludes the achievement of lower temperatures. Light from a titanium-sapphire laser is used to address the rubidium D1- and D2- resonances (near 377 THz and 384 THz, respectively). Due to the high pressure of the helium buffer gas, the resonances are broadened to linewidths of a few nanometer. Nevertheless, we may treat the rubidium atoms as laser-driven two-level atoms at the chosen (D-line) transition.